Computational investigation of the effect of biodiesel fuel properties on diesel engine NOx emissions

Wenqiao Yuan[1], A. C. Hansen[2]

(1. *Department of Biological and Agricultural Engineering, Kansas State University, Manhattan, KS* 66506, *USA*;
2. *Department of Agricultural and Biological Engineering, University of Illinois, Champaign, IL* 61801, *USA*)

Abstract: A detailed numerical spray atomization, ignition, combustion and nitrogen oxides (NOx) formation model was developed for direct injection diesel engines by using KIVA3V code. Several modified or recalibrated sub-models including a Kelvin-Helmholtz Rayleigh-Taylor (KH-RT) spray breakup model, a Shell ignition model, a single-step kinetic combustion model and a Zel'dovich NOx formation model were incorporated into KIVA3V. This modified model was validated by experimental data obtained from a John Deere 4045T direct injection diesel engine that was fueled with a natural soybean methyl ester, a yellow grease methyl ester, a genetically modified soybean methyl ester and No.2 diesel fuel. Errors between predictions of the brake-specific NOx and measured values were less than 1% at full load. For biodiesel fuels, either the Zel'dovich mechanism overpredicted NOx emissions, the ratio of NO to NOx should be less than diesel fuel, or both. As observed from the modeling results, the higher latent heat of vaporization and higher surface tension of biodiesel relative to diesel fuel did not result in increased NOx emissions. The higher viscosity of biodiesel could be one of the reasons for increased NOx, but its effect was relatively small compared with the effect of decreased spray cone angle and advanced start of injection timing on NOx. Decreased spray cone angle and advanced start of injection were the main reasons for increased NOx emissions of biodiesel.

Keywords: biodiesel, diesel engine modeling, NOx emissions

DOI: 10.3965/j.issn.1934-6344.2009.02.041-048

Citation: Wenqiao Yuan, A C Hansen. Computational investigation of the effect of biodiesel fuel properties on diesel engine NOx emissions. Int J Agric & Biol Eng, 2009; 2(2): 41－48.

1 Introduction

Biodiesel has gained considerable attention and support in the past few years, as demonstrated by its commercial availability in many parts of the United States and the provision of federal and state tax incentives that encourage its use. It is a bio-based fuel that can reduce net production of CO_2 from combustion sources and U.S. dependence on foreign oil. Biodiesel is a renewable fuel typically derived from vegetable oils or animal fats; therefore, its adoption as an alternative to fossil fuels would benefit and expand agricultural commodity markets. Biodiesel is of particular interest to the automobile industry and other areas in energy and environment because it is free of sulfur and has low emissions of particulate matter (PM), unburned hydrocarbons (HC) and carbon monoxide (CO) from combustion sources without modifications to existing diesel engines. Biodiesel is also the only alternative fuel that has passed the U.S. Environmental Protection Agency (EPA)-required Tier I and Tier II Health Effects testing requirements of the Clean Air Act Amendments of 1990.

One prominent negative aspect of biodiesel combustion is an increase in NOx emissions, including

Received date: 2009-02-04 **Accepted date**: 2009-06-10

Biographies: Wenqiao Yuan, Ph.D., Assistant Professor, majoring in biological and agricultural engineering, biofuels. Department of Biological and Agricultural Engineering, Kansas State University, Manhattan, KS 66506, USA. Tel: +1 785 532 2745; fax: +1 785 532 5825. Email: wyuan@ksu.edu. **A. C. Hansen, PhD,** Associate Professor, University of Illinois at Urbana Champaign, 360S AESB, MC-644, 1304 W. Pennsylvania Avenue, Urbana, IL 61801, USA, achansen@uiuc.edu

NO and NO_2, from some biodiesel fuels[1-3]. Most reported research on this issue focused only on experimental studies. Fundamental principles of the NOx increase are still unclear. This has motivated interest in modeling spray, ignition, combustion and NOx formation of biodiesel.

The objectives of this research were to (1) develop a detailed numerical spray atomization, ignition, combustion and NOx formation model for direct injection diesel engines by using KIVA3V code that could be applied to simulate combustion and predict NOx emissions of biodiesel fuels; (2) predict NOx emissions of a natural soybean oil methyl ester (SME), a yellow grease methyl ester (YGME), a genetically modified soybean methyl ester (GMSME) and No.2 diesel (D2) in a direct injection (DI) diesel engine; and (3) study the effect of latent heat of vaporization, viscosity and surface tension of biodiesel fuels on NOx emissions.

2 Fuel property predictions

Several properties of biodiesel fuels—critical temperature, normal boiling point, enthalpy, vapor pressure, latent heat of vaporization, viscosity and surface tension—are required inputs for combustion modeling. Some of these properties are temperature dependent and need to cover a wide temperature range from 0 K to the critical temperature of the fuel. A computer program, BDProp1.0, developed by Yuan et al.[4] was used to predict all required properties. Table 1 gives a brief description of methods that were integrated into this computer program. Detailed information concerning these methods was reported elsewhere[5-9].

Table 1 Fuel properties prediction methods

Properties	Methods
Critical Properties	Joback modification of Lydersen's method and Ambrose's method [5]
Latent Heat of Vaporization	Pitzer acentric factor correlation method [5]
Normal Boiling Point	Method by Yuan et al. [6]
Viscosity	Method by Yuan et al. [7]
Surface Tension	Method by Allen et al. [8]
Vapor Pressure	Method by Yuan et al. [6]
Heat of Formation	Method of Benson. [9]
Enthalpy	Method of Benson. [9]

3 KIVA computational models

KIVA-3V is a fully three-dimensional fluid dynamics model for chemically reacting flows[10]. Its sub-models were originally developed for petroleum-based fuels, such as gasoline and diesel. Few reports exist on KIVA-3V applications for biodiesel. This section briefly presents the models that were modified, recalibrated or added to KIVA-3V to include biodiesel in the fuel library.

3.1 Spray breakup model

The Kelvin-Helmholtz Rayleigh-Taylor (KH-RT) model[11] was applied for spray breakup in this study. The basis of this model was the concept introduced by Reitz and Diwakar[12] that atomization of the injected liquid and the subsequent breakup of drops are indistinguishable processes within a dense spray. The liquid injection was simulated by using the "blob" injection method[12], and the wave model[13] was used to simulate droplet breakup due to shear flow. In addition to the K-H type instability, Ricart et al.[11] suggested that the R-T instability might also play an important role because liquid droplets experience very high initial velocities and rapidly decelerate because of drag forces.

In the overall model, the K-H and R-T sub-models compete to break up the droplet[11]. The K-H model compared the wavelength with the droplet radius. If the wavelength was smaller than the droplet radius, the model assumed the wave was growing on the surface of the droplet, and the time of the growth was tracked and compared with the breakup time. Once the time was greater than the breakup time, the R-T breakup occurred. The K-H model was activated whenever the droplet radius was greater than the K-H wavelength.

The KH-RT model was originally developed for diesel engines fueled by petroleum diesel fuels. However, it is a physically based model, which means it can be extended to other fuels provided the physical properties are well defined. This is the reason we apply this model to the breakup of the sprays of both biodiesel and diesel fuels. Details of this model can be found in a previous publication[14].

3.2 Shell autoignition model

Among the parameters in diesel engine operation, ignition delay is considered critical to both performance and emissions from diesel engines. During the delay period, injected fuel undergoes a series of complex processes such as atomization, collision, vaporization and preliminary chemical reactions. Several approaches have been used to model the autoignition phenomena in multidimensional modeling of diesel engines with diesel fuels. Among these approaches, single-step irreversible Arrhenius kinetics models are often used because it is easy to apply the models in computational fluid dynamics (CFD) codes, and the results are reasonably accurate when some parameters are adjusted for different engine operating conditions. However, this model is not able to simulate the low-temperature autoignition process accurately in diesel engine conditions. This motivated interest in multistep models. The Shell model[15] is one of the multistep kinetics models that have been used by many researchers. The Shell model is an eight-step chemical kinetics model that involves some necessary generic reactions to simulate the controlling elementary reactions (i.e., initiation, propagation, branching and termination). Successful application of the Shell model to diesel engines can be found in several publications[16-18]. Eight generic reactions based on the degenerate branching characteristics of HC autoignition were formulated with five generic species and modified to account for differences between biodiesel and diesel. The model was described in more detail in a previous study[19].

3.3 Combustion model

The modified Shell ignition model was combined with the single-step kinetic combustion model, which has a reaction rate given by the following equation.

$$\text{Rate}= A_{fr,i}[\,fuel]^m[O_2]^n \exp(-E_i / RT) \qquad (1)$$

where m = 0.25 and n = 1.5 for both diesel and biodiesel; A_{fr} is the forward reaction rate coefficient, which is fuel and engine dependent and needs to be adjusted to match experimental data for each fuel; E is the activation energy (kJ/mol) of the fuels. Constants in the Shell ignition model were the same for all these fuels, but $A_{fr,1}$ and E_1 ($A_{fr,i}$ and E_i in eq.1 where i = 1, which is the fuel oxidization reaction) in the combustion model were different for each fuel. A_{f1} has a substantial effect on combustion[20]. If A_{f1} is too large, the KIVA combustion simulation will fail because of a too-high reaction rate. If A_{f1} is too small, the combustion cannot be sustained. A_{f1} can be determined only empirically. Once defined, it will be constant for all cases in the same engine with the same fuel. In this study, A_{f1} was 3.0×10^{11} and 4.5×10^{11} for diesel and biodiesel fuels, respectively. Activation energy of diesel fuel, E_1 of eq.1, was 1.578×10^4. To account for fuel cetane number, Ayoub[21] suggested that in the diesel engine ignition process, activation energy E_1 should be modified by a factor of 71.3/(CN+25), where CN denotes the cetane number of the fuel when the baseline D2 had a CN of 46.3. We changed the factor to 67.2/(CN+25) and applied it to the biodiesel combustion process. With the baseline D2 CN of 42.2, the factor is unity. For biodiesel fuels, $E_1=1.578\times10^4\times67.2/(CN+25)$.

3.4 NOx formation model

The extended Zel'dovich mechanism is implemented in KIVA-3V to describe NO formation. It is generally accepted that the principal reactions governing the formation of NO are[22]:

$$O + N_2 = NO + N \qquad (2)$$

$$N + O_2 = NO + O \qquad (3)$$

$$N + OH = NO + H \qquad (4)$$

The rate of formation of NO via reactions 2 to 4 is given by the following equation:

$$\frac{d[NO]}{dt} = k_1^+[O][N_2] + k_2^+[N][O_2] + k_3^+[N][OH] - k_1^-[NO][N] - k_2^-[NO][O] - k_3^-[NO][H] \qquad (5)$$

where the forward and reverse rate constants (k_i^+ and k_i^-, respectively) for each reaction are defined by Arrenius type equations as:

$$k_i^+ = A_{fr,i} \exp(-E_{f,i} / RT) \qquad (6)$$

$$k_i^- = A_{br,i} \exp(-E_{b,i} / RT) \qquad (7)$$

The forward and backward pre-exponential rate constants ($A_{fr,i}$ and $A_{br,i}$, respectively) and the forward and

backward reaction activation energy ($E_{f,i}$ and $E_{b,i}$, respectively) are suggested in the KIVA-3V manual[10]. R and T denote the universal gas constant (J/mol-K) and temperature (K). This extended Zel'dovich mechanism can predict only NO formation. In diesel engines, the NO_2 can be 10% to 30% of the total exhaust oxides of nitrogen emissions[22]. NO formed in the flame zone can be converted rapidly to NO_2 via the reaction with HO_2[22]:

$$NO + HO_2 \rightarrow NO_2 + OH \quad (8)$$

NO_2 can also be converted to NO by reacting with elemental oxygen:

$$NO_2 + O \rightarrow NO + O_2 \quad (9)$$

The above reaction does not occur when NO_2 formed in the flame is quenched by mixing with cooler fluid[22]. The NOx formation that includes both NO and NO_2 is formulated as:

$$\left(\frac{dNOx}{dt}\right)_{predicted} = \alpha \times \beta \times \left(\frac{dNO}{dt}\right)_{zel'dovich} \quad (10)$$

where α is a calibration factor introduced to calibrate the computed NOx with measured values, and β is a factor to convert NO to NOx. For engines fueled with diesel fuel, α=1.0 and β=1.533 (the ratio of the molecular weight of NO_2 to NO).

4 Model verification and application

Four biodiesel fuels—SME, YGME, GMSME and D2—were tested; their basic properties and fatty acid profiles are listed in Table 2. Other properties of the biodiesel fuels required for combustion modeling, such as critical temperature, enthalpy, vapor pressure, latent heat of vaporization, viscosity and surface tension were predicted on the basis of fatty acid profile by using BDPROP 1.0[4]. The molecular structure for D2 was $C_{12}H_{26}$, which was the recommended molecular structure for D2 used by the Cummins model in KIVA-3V. The molecular structure of SME, YGME and GMSME were $C_{19}H_{35}O_2$, $C_{18}H_{35}O_2$ and $C_{19}H_{36}O_2$, respectively. These molecular structures were defined from the fuel properties prediction model[4] to account for the actual carbon/hydrogen/oxygen ratio.

Table 2 Selected properties and fatty acid profile of No.2 diesel and biodiesel fuels

	D2	SME	YGME	GMSME
Carbon (% mass)	86.66	77.0	76.66	77.0
Hydrogen (% mass)	12.98	12.18	12.33	12.13
Sulfur (% mass)	0.034	<0.005	<0.005	<0.005
Oxygen (% mass by difference)	—	10.82	11.01	10.84
Nitrogen (ppm_m)	122	10	—	—
Cetane Number (ASTM D613)	42.2	50.4	62.6	—
Gross heat of combustion (kJ/kg)	45227	39968	40128	—
Net heat of combustion (kJ/kg)	42859	37383	37702	—
Kinematic viscosity (at 40°C, mm^2/s)	2.89	4.59	5.92	4.87
Specific gravity	0.8559	0.8796	0.8722	0.8750
C14:0	0	0	0.017	0
C16:0	0	0.1081	0.1947	0.0397
C16:1	0	0.0011	0	0.0013
C18:0	0	0.0454	0.1438	0.0299
C18:1	0	0.2496	0.5467	0.8254
C18:2	0	0.5066	0.0796	0.0498
C18:3	0	0.0727	0.0069	0.037
C20:0	0	0.0037	0.0025	0.003
C20:1	0	0.0032	0.0052	0.005
C22:0	0	0.0042	0.0021	0.0036
C24:0	0	0.0012	0	0.0012

4.1 Test engine

A John Deere 4045T diesel engine was tested, and the experimental data of cylinder pressure; injection pressure and injector needle lift; and exhaust emissions of CO, HC, NO and smoke along with engine working condition parameters (intake manifold temperature and pressure and exhaust temperature) were collected. Engine specifications are given in Table 3. For the CFD simulation, a 17×12×16 mesh was used for the 90° sector of the engine cylinder because this engine has four holes in each fuel injector. The mesh had 13675 cells and 13871 vertices.

Table 3 John Deere 4045T diesel engine specifications

Number of cylinders	4
Bore (mm)	106.5
Stroke (mm)	127.0
Connecting rod length (mm)	203.0
Compression ratio	17.0:1
Injector hole diameter (mm)	0.0315
Injector hole number	4
Maximum Power	66.5 kW at 2200 r/min
Peak Torque	374 N.m at 1200 r/min

4.2 Engine working conditions

Baseline engine conditions are listed in Table 4. The same engine speeds and loads were applied for each type of fuel tested. Intake air temperature and pressure for each test was about the same (Table 4). The increase in fuel consumption for biodiesel fuels is a result of their lower heat of combustion, which requires more fuel to maintain the same break torque as for D2. Variations in the start and end of injection for the three alternative fuels were brought about by the radial piston distributor type fuel injection system. An advance in the start of injection with increasing fuel delivery can be expected with this type of mechanical pump. The start of injection and end of injection were experimentally determined from the injector needle lift signal. The cause of earlier start of injection of GMSME than the other two biodiesel fuels is not clear.

Table 4 Baseline working conditions

	D2	SME	YGME	GMSME
Engine speed (r/min)	1400	1400	1400	1400
Brake torque (N.m)	352.5	352.5	353.2	354.5
Intake air temperature (K)	332.1	332.6	332.1	334.3
Intake air pressure (kPa)	125.978	124.599	125.978	124.999
Start of injection (CA)	-6.4	-7.13	-7.0	-7.8
End of injection (CA)	10.2	10.8	11.2	10.2
Fuel consumption rate (mg/cycle)	64.426	72.739	73.177	72.993
Maximum spray cone angle (degree)	47.5	30	30	45

Because of the confidence in the accuracy of NOx predictions from the models based on baseline cases, the authors tested more cases to study the effects of the fuel properties on NOx emission. The authors speculated that differences in properties, especially the latent heat of vaporization, viscosity and surface tension between biodiesel and diesel, might be a reason for increased NOx emissions of biodiesel. Therefore, the properties of SME were artificially changed from the original values for SME to the properties of D2. Two interceptions were applied as 67% SME with 33% D2 and 33% SME with 67% D2. Thus, the properties covered the range from SME to D2 with four cases, and more cases could be studied when needed. Working conditions of the engine were held identical to the baseline case of SME.

On the other hand, it is found from the sensitivity study that the initial maximum spray cone angles varied for different fuels. Biodiesel fuels had smaller spray cone angles (Table 4). Spray cone angle was determined as an adjustable parameter by matching predicted cylinder pressure with measured data. The smaller spray cone angles of biodiesel fuels were in good agreement with experimental observations by Senda et al.[23], but reasons for this phenomenon are still not clear. It could be related to differences in fuel properties (including surface tension and viscosity), and it also could be due to engine working conditions. The higher surface tension and viscosity of biodiesel fuels could reduce spray angle, and the earlier combustion could also suppress the spray cone to be formed. The GMSME had a bigger spray cone angle than the other two biodiesel fuels, which was probably due to its earlier injection timing, considering that earlier injection gave a longer time for the spray cone to be formed. Also, start of injection of biodiesel fuels was earlier than that of diesel fuel, which also had a significant effect on NOx emissions. To study the effect of spray cone angle and start of injection on NOx formation of biodiesel, we artificially set the spray cone angle to 31.5°, 41° and 47.5° and changed the start of injection timing to –7°, –6.7° and –6.4° crank angle (CA). These two parameters were adjusted from SME to D2. These changes were applied to SME baseline case while holding other parameters constant, and we believe the result should be duplicable for other types of biodiesel fuels.

5 Results and discussion

5.1 Selected fuel properties from prediction

The predicted latent heat of vaporization, viscosity and surface tension of D2 and biodiesel fuels are shown in Figures 1 to 3. These properties are important to the fuel spray process in the diesel engine combustion chamber. All three biodiesel fuels have higher latent heat of vaporization, viscosities and surface tensions than D2. Differences in latent heat of vaporization and surface tension among the biodiesel fuels are not significant, but YGME had higher viscosity than GMSME, and SME had the lowest viscosity.

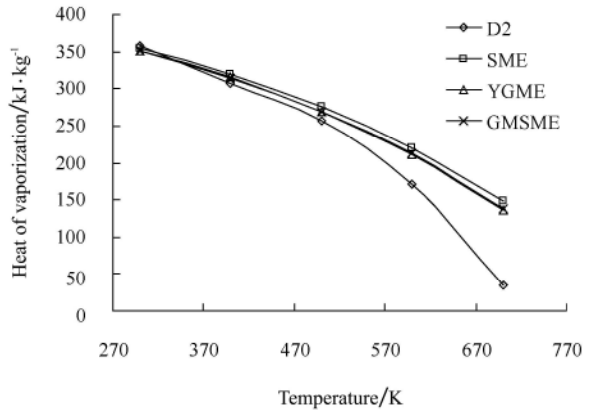

Figure 1 Predicted latent heat of vaporization

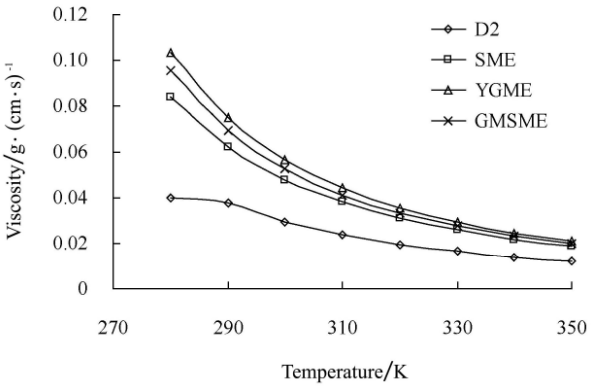

Figure 2 Predicted dynamic viscosities

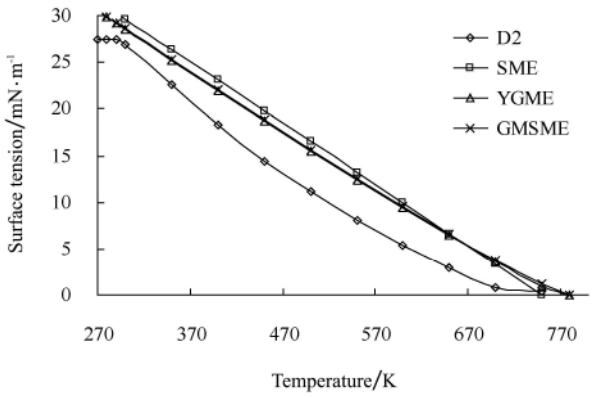

Figure 3 Predicted surface tension

5.2 NOx emissions of baseline cases

Measured and predicted brake-specific NOx (BSNOx) emissions for the baseline cases are shown in Table 5. With the calibration factor α = 1.0 and NO to NOx factor β = 1.533, NOx of the three biodiesel fuels were all overpredicted by more than 12%. This result shows that either the calibration factor, α, the NO to NOx factor, β, or both needed to be adjusted for biodiesel fuels. When α = 1.0 and β = 1.35 or α = 0.881 and β = 1.533 as shown in the parentheses in Table 5, prediction errors for all three biodiesel fuels were less than ±1%. That α = 0.881 (instead of 1.0) suggests that the NOx from Zel'dovich mechanism of biodiesel fuels were overpredicted. This overprediction could be due to the higher combustion temperature, as found in a previous study[14], or to overpredicted O_2 concentration in fuel/air mixture, assuming the oxygen in biodiesel has the same effect on NO formation as the O_2 in the air. The β = 1.35 instead of 1.533 indicates there was less NO_2 in the NOx exhaust emissions of biodiesel fuels than in emissions of D2. This could be explained by Reaction 9 because more oxygen atoms that come from the biodiesel molecule exist in the biodiesel/air mixture to convert NO_2 back to NO.

Table 5 Comparisons of predicted and measured brake specific NOx (BSNOx) emissions

	D2	SME	YGME	GMSME
Measured BSNOx (g/kW.h)	8.10	8.88	8.18	8.46
Predicted BSNOx (g/kW.h) (α=1.0, β=1.533)	8.10	10.03	9.176	9.7
Relative error (%)	0	12.95	12.18	14.66
Adjustment or Calibration				
Calibration factor (α)	1.0	1.0 (0.881)	1.0 (0.881)	1.0 (0.881)
NO to NOx factor (β)	1.533	1.35 (1.533)	1.35 (1.533)	1.35 (1.533)
Adjusted Predicted BSNOx (g/kW.h)	8.10	8.81	8.26	8.54
Relative error (%)	0	-0.79	0.98	0.95

5.3 NOx emissions of test cases

The predicted BSNOx emissions of SME for tested cases are shown in Table 6. For comparison, the baseline cases are also included in the same table (shaded cells). Because the maximum prediction error of the baseline cases is ±1%, any difference in predicted NOx greater than 2% was considered significant. When heat of vaporization decreased from that of pure SME to pure D2, NOx neither changed in one direction nor changed significantly (Table 6). This suggests the difference in heat of vaporization between biodiesel and diesel was not the cause of increased NOx, which is in agreement with experimental results from Tat and Van Gerpen[3]. When surface tension decreased from pure SME to D2, NOx did not change significantly, nor did it change in one direction. Therefore, we believe that surface tension did

not contribute to the increased NOx. When viscosity decreased from SME to D2, NOx decreased up to 3.52% but not proportionally. More cases were tested by adding one case between every two cases. Therefore, in addition to the SME case, six cases were studied for viscosities: 87% of SME + 13% of D2, 67% of SME + 33% of D2, 52% of SME + 48% of D2, 33% of SME + 67% of D2, 17% of SME + 83% of D2 and D2. All six cases had lower NOx than SME, but it seemed there was a NOx neutral case between SME and D2. When viscosities decreased from SME to D2, NOx decreased first, then reached the NOx level that was the same as that of SME and then decreased again, indicating that the higher viscosity of biodiesel fuels could be one of the reasons for increased NOx. However, the corresponding mechanisms have yet to be determined. Two more cases were studied by giving the viscosities of GMSME and YGME to SME to determine whether the higher viscosities of GMSME and YGME affected NOx. No significant effect of these higher viscosities on NOx was found.

In addition, both the spray cone angle and start of injection timing had a significant effect on NOx emissions (Table 6). With increased spray cone angle or retarded start of injection, BSNOx decreased significantly. One possible explanation of the effect of spray angle on BSNOx is that the decreased spray cone angle of biodiesel increases spray penetration, as observed in experimentation by Senda et al.[23]. This, consequently, increases the degree of widespread combustion in the engine combustion chamber, which increases NOx emissions. It must be noted that KIVA-3V cannot predict spray cone angle. Spray cone angle is an input parameter in KIVA-3V that has to be determined either experimentally or by matching cylinder pressure like in this study. The effect of injection timing on BSNOx is well known as advanced injection of biodiesel increases the combustion temperature that favors NOx formation. By adjusting either the spray cone angle or injection timing, BSNOx of SME can be achieved to the level of D2. Therefore, we conclude that decreased spray cone angle and advanced start of injection were the main reasons for increased NOx emissions of biodiesel.

Table 6 Predicted brake specific NOx (BSNOx) of SME

Property (values at the reference temperatur) or parameter	Predicted BSNOx (g/kWh)	Relative difference/%
Heat of vaporization		
100% SME (205.1 kJ/kg at 620K)	8.81	
67% SME + 33% D2 (185.1 kJ/kg at 620K)	8.67	-1.59
33% SME + 67% D2 (164.5 kJ/kg at 620K)	8.89	0.91
100% D2 (144.5 kJ/kg at 620K)	8.82	0.11
Viscosity		
100% SME (3.588 cP at 40°C)	8.81	
67% SME + 33% D2 (3.148 cP at 40°C)	8.60	-2.38
33% SME + 67% D2 (2.694 cP at 40°C)	8.80	-0.11
100% D2 (2.253 cP at 40°C)	8.50	-3.52
83% SME + 17% D2 (3.361 cP at 40°C)	8.60	-2.38
52% SME + 48% D2 (2.947 cP at 40°C)	8.78	-0.34
17%SME + 83%D2 (2.48 cP at 40°C)	8.65	-1.82
=GMSME viscosity (3.857 cP at 40°C)	8.82	0.11
=YGME viscosity (4.131 cP at 40°C)	8.87	0.68
Surface tension		
100% SME (28.12 mm2/s at 40°C)	8.81	
67% SME + 33% D2 (27.34 mm2/s at 40°C)	8.69	-1.36
33% SME + 67% D2 (26.54 mm2/s at 40°C)	8.77	-0.45
100% D2 (25.76 mm2/s at 40°C)	8.88	0.79
Spray cone angle		
30°	8.81	
35°	8.78	-0.35
41°	8.08	-8.59
47.5°	7.52	-15.18
Start of injection		
7.13 BTDC	8.81	
7.0 BTDC	8.34	-5.53
6.7 BTDC	8.09	-8.47
6.4 BTDC	7.72	-12.82

6 Conclusions

Several sub-models have been incorporated into KIVA3V. These sub-models include a KH-RT spray breakup model, a Shell ignition model, a single-step kinetic combustion model and a Zel'dovich NOx formation model that have been modified or calibrated for biodiesel. The modified KIVA3V model was applied to a John Deere 4045T direct-injection diesel engine fueled by SME, YGME, GMSME, and D2 to predict NOx emissions from the engine. Predictions of BSNOx were compared with measured values from this engine, and errors were less than ±1%. For biodiesel fuels, either the Zel'dovich mechanism over-predicted NOx emissions, the ratio of NO to NOx should be less than diesel fuel, or

both.

As observed from the modeling results, the higher latent heat of vaporization and higher surface tension of biodiesel relative to diesel fuel were not the leading reason for increased NOx emissions. The higher viscosity of biodiesel could be one of the reasons for increased NOx, but its effect was relatively small compared with the effect of decreased spray cone angle and advanced start of injection timing. Decreased spray cone angle and advanced start of injection were the main reasons for increased NOx emissions of biodiesel.

Acknowledgments

This material is based on work supported by the U.S. Department of Agriculture Cooperative State Research, Education, and Extension Service under Project No. Hatch 10-311 AE. Financial support was also provided by the Kansas Agricultural Experiment Station (Contribution No. 09-232-J from the Kansas Agricultural Experiment Station).

[References]

[1] McCormick R L, Graboski M S, Herring A M, Alleman, T L. Impact of biodiesel source material and chemical structure on emissions of criteria pollutants from a heavy-duty engine. Environmental Science & Technology, 2001; 35(9): 1742－1747.

[2] Grimaldi C N, Postrioti L, Battistoni M, Millo, F. Common rail HSDI diesel engine combustion and emissions with fossil/bio-derived fuel blends. 2002. SAE technical paper 2002-01-6085.

[3] Tat M, Van Gerpen J H. Fuel property effects on biodiesel. ASAE, St. Joseph, MN. 2003. ASAE Paper No. 036034.

[4] Yuan W, Hansen A C, Zhang Q. Prediction of biodiesel fuel properties based on fatty acid composition. ASAE, St. Joseph, MN. 2004. ASAE Paper No. 046086.

[5] Yuan W, Hansen A C, Zhang Q. Predicting the physical properties of biodiesel for combustion modeling. Trans. ASABE, 2003; 46(6): 1487－1493.

[6] Yuan W, Hansen A C, Zhang Q. Vapor pressure and normal boiling point predictions for pure methyl esters and biodiesel fuels. Fuel, 2005; 84(7-8): 943－950.

[7] Yuan W, Hansen A C, Zhang Q. Temperature dependent kinematic viscosity of biodiesel fuels and blends. Journal of American Oil Chemists Society, 2005; 82(3): 195－199.

[8] Allen C A W, Watt, K C, Ackma, R G. Predicting the surface tension of biodiesel fuels from their fatty acid composition. Journal of American Oil Chemists' Society. 1999; 76(3): 317－323.

[9] Yuan W, Hansen A C, Zhang Q. Prediction of biodiesel fuel properties based on fatty acid composition. ASABE Paper No. 046086. Ottawa, Canada: ASABE, 2004.

[10] Amsde A A. KIVA-3V: A Block-structured KIVA program for rngines with vertical or canted valves. Los Alamos National Labs, LA-13313-MS. 1997.

[11] Ricart L M, Xin J, Bower G R, Reitz R D. In-cylinder measurement and modeling of liquid fuel spray penetration in a heavy duty diesel engine. SAE Technical Paper 971591.

[12] Reitz R D, Diwakar R. Structure of high pressure sprays. SAE Technical Paper 870598.

[13] Reid R D. Modeling atomization processes in high-pressure vaporizing sprays. Atomization and Spray Technology, 1987; 3, 309－337.

[14] Yuan W, Hansen A C, Tat M E, Van Gerpen J H, Tan Z. Spray, ignition and combustion modeling of biodiesel fuels in a DI diesel engine. Transactions of the ASABE, 2005; 48(3): 589－595.

[15] Halstead M P, Kirsch L J, Quinn C P. The autoignition of hydrocarbon fuels at high temperatures and pressure-fitting of a mathematical model. Combustion and Flame, 1977; 30, 45－60.

[16] Theobald M A, Cheng W K A. Numerical study of diesel ignition. Journal of the ASME. 1987, 87－FE-2.

[17] Kong S C, Reitz R D. Multidimensional modeling of diesel ignition and combustion using a multistep kinetics model. ASME Transactions, Journal of Engineering for Gas Turbines and Power, 1993; 115(4): 781－789.

[18] Hamosfakidis C, Reitz R D. Optimization of a hydrocarbon fuel ignition model for two single component surrogates of diesel fuel. Combustion and Flame, 2003; 132, 433－450.

[19] Yuan W, Hansen A C, Zhang Q. Computational study of biodiesel ignition in a direct injection engine. ASAE, St. Joseph, MN, 2003, ASAE Paper No. 036035.

[20] Amsden A A. KIVA-3: a KIVA program with block-structured mesh for complex geometries. Los Alamos National Labs, LA-12503-MS. 1993.

[21] Ayoub N, Modeling multicomponent fuel sprays in engines with application to diesel cold-starting. Ph.D. Dissertation, University of Wisconsin-Madison, 1995. Heywood J B. Internal Combustion Engine Fundamentals. McGraw-Hill Inc. New York, 1988.

[22] Senda J, Okui N, Suzuki T, Fujimoto H. Flame structure and combustion characteristics in diesel engines fueled with biodiesel. SAE technical paper, 2004-01-0084.